Analytical and numerical study of the Entropy Wave Generator experiment on indirect combustion noise

Ignacio Durán* — *CERFACS, Toulouse, 31057 France*

Stéphane Moreau† — *Université de Sherbrooke, Sherbrooke, J1K2R1, QC Canada*

When considering combustion as a noise source, two main mechanisms can be identified as responsible for its generation: direct combustion noise, in which acoustic waves generated by the flame propagate to the outlet, and indirect combustion noise (or entropy noise), in which entropy waves generate noise as they are accelerated with the mean flow through the turbine stages. The Entropy Wave Generator (EWG) experiment showed the importance of entropy noise in the supersonic and created a test-bench to validate analytical and numerical tools used to predict combustion noise. In this paper the subsonic case of this experiment is analysed, showing the influence of direct combustion noise and studying the validity of present analytical methods used to calculate the waves propagation through the nozzle.

Nomenclature

Latin letters

c	Fluid mean sound speed
C_p	Heat capacity at constant pressure
d	Characteristic slope length of the heating device
f	Frequency
i	Imaginary unit ($i^2 = -1$)
L^-	Entering wave at the outlet boundary
l_h	Heating device length
L_n	Nozzle length
L_{in}	Length of the inlet domain of the nozzle
L_{out}	Length of the exit domain downstream the nozzle throat
M	Mach number
m	Mass flow rate
p	Fluid pressure
p_2	Outlet pressure
p_{ref}	Reference static pressure at the outlet
Q'	Fluctuating heat release of the heating device
q'	Dimensionless fluctuating heat release of the heating device
R_1	Reflection coefficient at the inlet of the EWG nozzle, phase-shifted to the nozzle throat
R_2	Reflection coefficient at the outlet of the EWG nozzle, phase-shifted to the nozzle throat
R_{in}	Reflection coefficient at the inlet of the EWG nozzle, after the Settling Chamber
R_{out}	Reflection coefficient at the outlet of the experimental configuration
R_{sc}	Reflection coefficient at the inlet of the settling chamber

*Ph.D. candidate financed by SNECMA. ignacio.duran@cerfacs.fr, AIAA Member

†Professor, GAUS, Mechanical Engineering Department, AIAA Lifetime Member

s Fluid entropy
S_0 Cross-section area of the nozzle inlet
S_{sc} Cross-section area of the Settling chamber
t Time
t_0 Time of the heating device triggering
T_p Heating device's pulse duration
T_t Fluid total temperature
u Fluid velocity
w^+ Acoustic wave propagating downstream
w^- Acoustic wave propagating upstream
w^s Entropy wave
x Axial coordinate of the nozzle
x_0 Heating device location

Greek Letters

Δt Time step of the numerical simulation
η Indirect to direct noise ratio at the outlet
Γ Cross-section area ratio ($= S_0/S_{sc}$)
γ Specific heats ratio
κ Relaxation coefficient on pressure at the outlet boundary condition
λ Characteristic acoustic wavelength
Ω Dimensionless frequency
ω Angular frequency
$\phi(t)$ Temporal variation of the electrical device source term
$\phi(x,t)$ Source term in the energy equation
Φ_0 Amplitude of the source term in the energy equation
ρ Fluid mean density
τ Relaxation time of the heating device pulse model

I. Introduction

Noise emissions are a major issue for aircraft and engines manufacturers due to the proximity of airports to residential zones and mostly as international regulations are becoming more and more strict in that aspect. During the last decades, research efforts have been made, permitting a significant reduction of jet, fan and external aerodynamic noise. This reduction has to be continued in order to meet future norms. The reduction of these sources has increased the relative influence of other noise sources in the aircraft. For these sources the possible reduction is relatively high, as physical mechanisms governing them are not yet fully understood. One of these sources is combustion noise, which is generated by heat fluctuations induced by the turbulent flame. These fluctuations generate acoustic and entropy waves that propagate through the turbine stages to reach the outlet of the engine, contributing to the global engine noise. This noise source has been identified as significant at take-off, when the engine is at its full power.

Two mechanisms of combustion noise generation can be identified: Direct combustion noise, which is due to acoustic waves generated in the combustion chamber that propagate through the turbine stages reaching the outlet, and indirect noise, which appears when entropy waves (hot spots) are accelerated through the turbine. The acceleration of these entropy waves generates pressure fluctuations which propagate upstream (contributing to combustion instabilities when a positive feedback occurs), and downstream from the turbine stage (generating combustion noise). Both mechanisms of combustion noise generation were shown by Marble and Candel[12] using the Linearised Euler Equations (LEE) and developing an analytical method to solve the propagation equations considering a quasi-1D configuration, based on the compact nozzle hypothesis. This hypothesis was used to extend the analytical method to a 2D configuration of a turbine stage (Cumpsty and Marble[5]). The study of combustion noise is directly linked to the propagation of acoustic and entropy waves through the turbine stages, where the mean flow is accelerated and decelerated repeatedly. While the propagation of noise in the free medium has been studied in depth ([1,4,6,11]),

no acoustic analogy exists for the propagation of acoustic and entropy waves through turbo-machinery. Instead, the one-dimensional and two-dimensional models of waves propagation can be used to propagate the noise generated to the outlet of the engine. It is important to validate this model: waves generated in the combustion chamber can be simulated using advanced Large Eddy Simulations (LES) and, combining them with the analytical model of waves propagation, the noise at the outlet can be predicted. This can be done without having to combine LES with a turbine stage simulation, which would be extremely CPU demanding.

Leyko *et al.*[10] used the one dimensional analytical method combined with numerical tools to show that the ratio of indirect to direct combustion noise is high in actual aero-engines, but low in most laboratory combustion chambers. This is due to the fact that combustion chambers in laboratories are not followed by a strong mean flow acceleration, and therefore indirect noise is negligible in those configurations. Out of all the experiments performed up to now concerning combustion noise, the one performed by Bake *et al.*[3] is at the moment the only one focused specifically on indirect combustion noise. This experiment, called the Entropy Wave Generator (EWG) (described in Section II), was used by Leyko *et al.*[9] to validate the analytical tools created by Marble and Candel[12] in the supersonic case, showing that indirect combustion noise can be correctly predicted using the analytical method. In this work we will focus on the subsonic case to explain the mechanisms generating noise in the EWG experience and to analyse the compact nozzle hypothesis in the subsonic case.

This paper is structured as follows: In Section II the experimental configuration of the EWG experiment is described. A numerical simulation of the complete set-up is performed in Section III. The fully analytical method of Marble and Candel[12] is described and discussed in Section IV, followed by a first order analysis of the indirect to direct combustion noise ratio (Section V). A semi-analytical method to solve the wave propagation through the nozzle without the compact nozzle hypothesis is presented in Section VI. Finally, conclusions are presented in Section VII.

II. The EWG experiment configuration

The experiment performed by Bake *et al.*[3] at the DLR consists of a convergent-divergent nozzle with an electrical heating device placed at the inlet as shown in Fig 1. Main geometrical parameters are summarized in Table 1. The operating conditions can be varied from the unchoked configuration to choked flow with various exit Mach numbers, depending on the mass flow rate. Leyko *et al.*[9] already studied the supersonic case (with a normal shock at the divergent). The present study is therefore restricted to the unchoked configuration, using mainly Reference Test Case 2 of,[3] summarized in Table 2 .

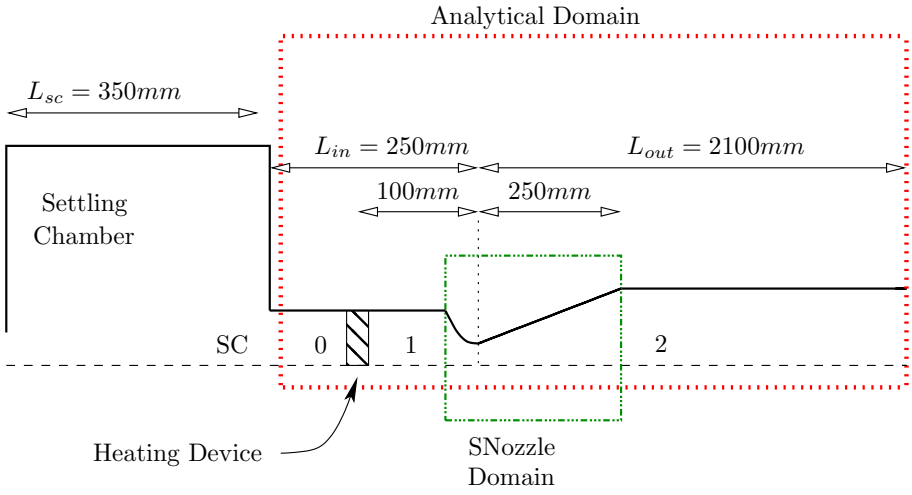

Figure 1. Sketch of the EWG with the definition of the analytical and the SNozzle domains, and the sections where the different variables will be calculated: SC, 0, 1 and 2.

The mean steady flow is perturbed with a temperature pulse (shown in Fig 2), generated electrically at

Convergent Length	Divergent Length	Inlet Diameter	Outlet Diameter	Throat Diameter
13mm	250mm	30mm	40mm	7.5mm

Table 1. Geometric characteristics of the experimental set-up

Inlet Mach number	Throat Mach Number	Outlet Mach number	Inlet Pressure	Outlet Pressure
0.033	0.7	0.01861	105,640Pa	101,300Pa

Table 2. Physical parameters of the subsonic case (Reference Test Case 2)

the inlet with a period of 1 second. This pulse is convected through the nozzle throat, generating acoustic waves which are measured using four microphones placed at different sections at the outlet. For the study presented here, the microphone placed at a distance of 1150 mm downstream from the nozzle throat will be used to compare the analytical and numerical results with the experiment.

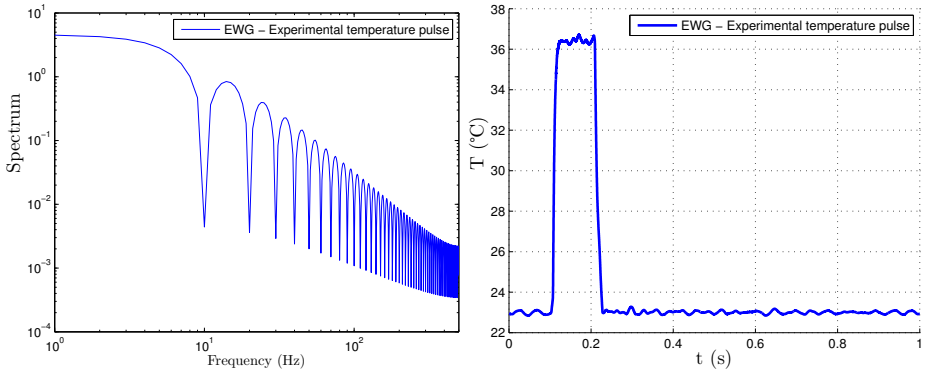

Figure 2. Experimental temperature pulse induced by the heating device. Left: spectrum. Right: time signal.

III. Numerical simulations

Numerical simulations were performed using the code AVBP developped at CERFACS[15] to reproduce the experimental results. As in,[9] 3D effects are negligible in this case, and therefore an axisymmetric mesh is enough to capture completely the noise generated by the heating device. The considered geometry takes into account the complete nozzle, including the settling chamber (Fig. 1).

The maximal mesh size is 1 mm, enough to resolve the temperature pulse accurately. Lax-Wendroff scheme is used to perform the simulations, using Euler equations (therefore no viscosity, turbulence or boundary layers are taken into account in order to isolate combustion noise from other possible sources).

The heating device is simulated as a source term in the energy equation. The energy is distributed spatially,

$$\phi(x,t) = \Phi_0 \frac{1}{2}\left[\tanh\left(\frac{x-x_0+l_h/2}{d}\right)\tanh\left(-\frac{x-x_0-l_h/2}{d}\right)+1\right]\phi(t) \quad , \tag{1}$$

where x_0 is the heating device location, l_h the heating device length, d a characteristic slope length and $\phi(t)$ the temporal fluctuation of the source term, given by an analytical function approximating the pulse

generated, as done by Leyko *et al.*,[9]

$$\phi(t) = \begin{cases} 1 - \exp(\frac{t-t_0}{\tau}) & \texttt{if} \quad t \in [t_0, t_0 + T_p] \\ \\ \phi(t_0 + T_p)\exp(-\frac{t-t_0}{\tau}) & \texttt{if} \quad t > t_0 + T_p \end{cases} \quad , \tag{2}$$

where t_0 is the triggering time, $T_p = 100$ ms the pulse duration and τ the relaxation time of the pulse, set to 7 ms in our case. The comparison of the experimental and the analytical temperature pulse is shown in Fig. 3 .

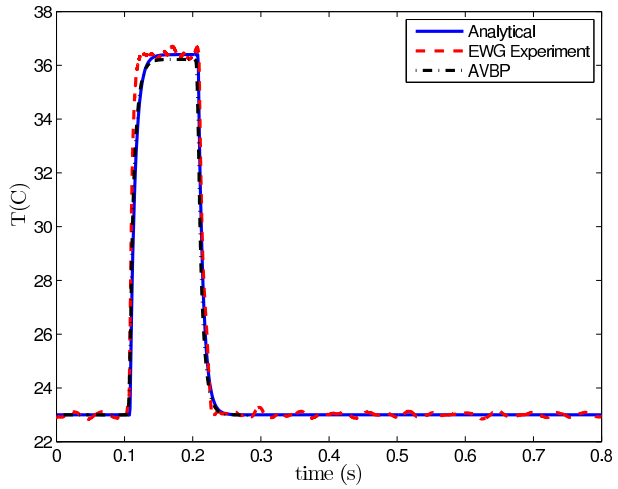

Figure 3. Experimental temperature pulse induced by the heating device. Analytical function modelling the temperature signal compared to the EWG experimental data

A. Inlet and outlet reflection coefficients

Special care should be taken with the boundary conditions. Leyko *et al.*[9] showed during the study of the supersonic case that reflecting conditions should be considered at the outlet to mimic the experimental set-up correctly. The reflecting properties of the experiment were measured (Mühlbauer *et al.*[13]) and it was found that they can be reproduced using a first order filter, namely,

$$R_{out} = \frac{-1}{1 + 2\imath\omega/\kappa} \quad . \tag{3}$$

This first order filter can be introduced in the computation without having to modify the code using non-reflecting boundary conditions (Poinsot and Lele[14]). This formulation of the boundary condition imposes the incoming waves as a function of the difference between the local and the reference pressures, namely,

$$L^- = 2\kappa\Delta t(p_{ref} - p_2)/(\rho c) \quad . \tag{4}$$

When considering $\kappa = 0$ the boundary is completely non-reflecting, and when $\kappa \to \infty$ waves are completely reflected. For any intermediate value, the boundary condition acts as the first order filter of Eq. 3. This boundary condition is imposed at the outlet of the computational domain. Both the length of the nozzle in the computational domain and the value of κ have to be tuned using the experimental data to reproduce the correct boundary condition. This was already done by Leyko *et al.*[9] for the supersonic case, obtaining $\kappa = 160\ s^{-1}$ and $L_{out} = 2100$ mm measured from the nozzle throat. The outlet reflection coefficients are plotted in Fig 5 of,[9] where the experimental data is compared with the first order filter.

As the computational domain takes into account the settling chamber, the inlet reflection coefficient of the nozzle is included in the simulation, and no modelling is needed. For the inlet of the settling chamber a fully reflecting inlet mass flow is used.

These values of the reflection coefficients were already used by Leyko *et al.*[9] to reproduce correctly the indirect noise measurements in the supersonic case.

B. Numerical Results

Results of the numerical simulations plotted in Fig. 4 compared to the experimental data show that the general shape is captured. To obtain a perfect match in the shape, a better model for the reflection coefficient should be used instead of a first order filter modelization.

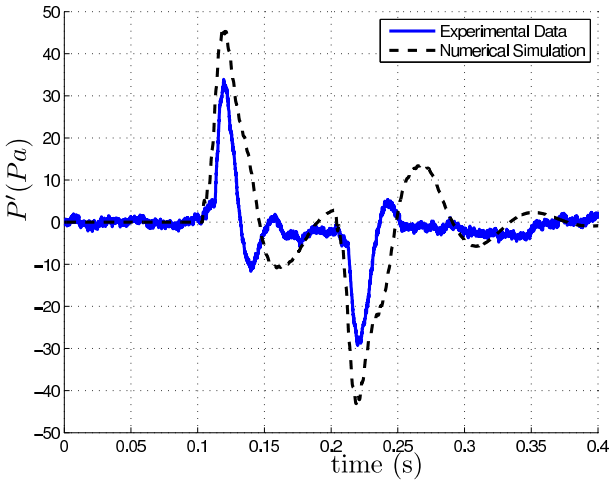

Figure 4. Numerical simulation pressure signal compared to experimental data from the EWG

Results show that the noise generated in the EWG cannot be calculated with this analytical tool taking into account only the direct noise contribution. It also shows the important contribution of the reflection coefficients in the result obtained.

IV. Fully analytical approach

To solve the propagation of acoustic and entropy waves, the quasi-1D linearised Euler equations (LEE) are written as in,[12]

$$\left[\frac{\partial}{\partial t}+u\frac{\partial}{\partial x}\right]\left(\frac{p'}{\gamma p}\right)+u\frac{\partial}{\partial x}\left(\frac{u'}{u}\right)=0 \quad , \tag{5}$$

$$\left[\frac{\partial}{\partial t}+u\frac{\partial}{\partial x}\right]\left(\frac{u'}{u}\right)+\frac{c^2}{u}\frac{\partial}{\partial x}\left(\frac{p'}{\gamma p}\right)+\left(2\frac{u'}{u}-(\gamma-1)\frac{p'}{\gamma p}\right)\frac{du}{dx}=\frac{du}{dx}\frac{s'}{C_p} \quad , \tag{6}$$

$$\left[\frac{\partial}{\partial t}+u\frac{\partial}{\partial x}\right]\left(\frac{s'}{C_p}\right)=0 \quad , \tag{7}$$

where non-primed variables u and p represent the mean flow velocity and pressure, and primed variables represent small fluctuations of speed u', pressure p' and entropy s'. C_p is the specific heat capacity and γ the heat capacity ratio. These equations contain the terms of acoustic wave propagation (direct noise) and the entropy noise generation (indirect noise). The indirect noise is caused by the last term of Eq. 6, where the entropy wave appears as a source term, which is non-zero when a mean flow gradient exists. It is important to notice that the amplitude of the indirect noise depends directly on the mean flow acceleration.

An analytical solution can be found for the LEE in the low frequency limit, as shown in.[12] This assumption (called compact nozzle hypothesis) states that the characteristic wavelength of the waves propagating through the nozzle (λ) is long compared to the nozzle length. In other words, the Helmholtz number (or non-dimensional frequency), written as,

$$\Omega = \frac{L_n}{\lambda} = \frac{f L_n}{c_1} \quad . \tag{8}$$

is negligible. $L_n = 263$ mm is the nozzle length, c_1 is the sound speed at the inlet of the nozzle (see Fig. 1) and f the frequency in Hz. For the case of the EWG experiment, it can be seen in Fig 2 that most of the spectral energy of the temperature pulse is contained at frequencies lower than 100 Hz, which gives a Helmholtz number of $\Omega \approx 0.077$. As the nozzle is considered short compared to the wavelength of the perturbations, the conservation equations of mass, enthalpy and entropy perturbations can be written between the inlet and the outlet, giving three jump conditions, namely,

$$\left(\frac{\dot{m}'}{\dot{m}}\right)_1 = \left(\frac{\dot{m}'}{\dot{m}}\right)_2 \quad , \tag{9}$$

$$\left(\frac{T_t'}{T_t}\right)_1 = \left(\frac{T_t'}{T_t}\right)_2 \quad , \tag{10}$$

$$\left(\frac{s'}{C_p}\right)_1 = \left(\frac{s'}{C_p}\right)_2 \quad . \tag{11}$$

Using isentropic relations, the ideal gas law, and writing the mass flow as $\dot{m} = \rho A u$, the mass, total temperature and entropy equations can be written as a function of the primitive variables p, u and s, namely,

$$\frac{\dot{m}'}{\dot{m}} = \frac{1}{M}\frac{u'}{c} + \frac{p'}{\gamma p} - \frac{s'}{C_p} \quad , \tag{12}$$

$$\frac{T_t'}{T_t} = \frac{1}{1 + [(\gamma-1)/2]M^2}\left[(\gamma-1)M\frac{u'}{c} + (\gamma-1)\frac{p'}{\gamma p} + \frac{s'}{C_p}\right] \quad , \tag{13}$$

$$\frac{s'}{C_p} = \frac{p'}{\gamma p} - \frac{\rho'}{\rho} \quad , \tag{14}$$

to have a system of equations relating the primitive variables at the inlet and at the outlet of a compact element.

To correctly impose the boundary conditions, equations 12-14 should be written as a function of the three considered waves,

$$w^+ = \frac{p'}{\gamma p} + \frac{u'}{c} \quad , \tag{15}$$

$$w^- = \frac{p'}{\gamma p} - \frac{u'}{c} \quad , \tag{16}$$

$$w^s = \frac{s'}{C_p} = \frac{p'}{\gamma p} - \frac{\rho'}{\rho} \quad , \tag{17}$$

which corresponds to the downstream and upstream propagating acoustic waves and the entropy wave, propagating at speeds $u + c$, $u - c$ and u respectively.

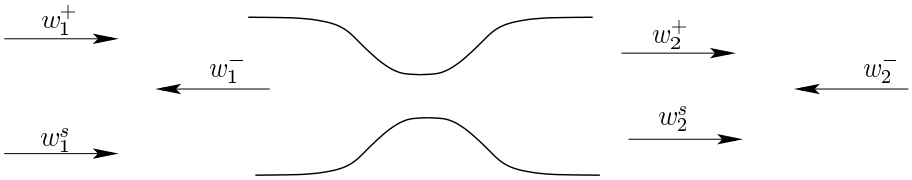

Figure 5. Acoustic and entropy waves at the nozzle inlet and outlet in a subsonic nozzle

Doing so, and writing the conservation of the invariants between the inlet and the outlet, three relations between the incoming and out-coming waves can be written,

$$(1 + \frac{1}{M_1})w_1^+ + (1 - \frac{1}{M_1})w_1^- = (1 + \frac{1}{M_2})w_2^+ + (1 - \frac{1}{M_2})w_2^- \quad , \tag{18}$$

$$\frac{(1+M_1)w_1^+ + (1-M_1)w_1^- + \dfrac{2w_1^s}{\gamma-1}}{1+\dfrac{\gamma-1}{2}M_1^2} = \frac{(1+M_2)w_2^+ + (1-M_2)w_2^- + \dfrac{2w_2^s}{\gamma-1}}{1+\dfrac{\gamma-1}{2}M_2^2}, \tag{19}$$

$$w_1^s = w_2^s \quad . \tag{20}$$

For the subsonic case, three waves are incoming (w_1^+, w_1^s and w_2^-) and have to be imposed, and three are out-coming, and therefore unknown (w_1^-, w_2^+ and w_2^s), as seen in Fig. 5 . The problem can be solved using only the three relations of Eq 18-20. A matrix system can be written to solve the problem, considering only indirect noise and both reflection coefficients at the inlet and outlet of the nozzle R_1 and R_2, namely,

$$\begin{bmatrix} \xi_1^+ R_1 + \xi_1^- & -(\xi_2^+ + \xi_2^- R_2) \\ \zeta_1(\beta_1^+ R_1 + \beta_1^-) & -\zeta_2(\beta_2^+ + \beta_2^- R_2) \end{bmatrix} \begin{bmatrix} w_1^- \\ w_2^+ \end{bmatrix} = \begin{bmatrix} 0 \\ \zeta_2 - \zeta_1 \end{bmatrix} w_1^s \quad , \tag{21}$$

where ξ, β and ζ are a function of the Mach number only,

$$\xi^{\pm} = 1 \pm \frac{1}{M} \quad , \tag{22}$$

$$\beta^{\pm} = \frac{\gamma-1}{2}(1 \pm M) \quad , \tag{23}$$

$$\zeta = \left(1 + \frac{\gamma-1}{2}M^2\right)^{-1} \quad . \tag{24}$$

The reflection coefficients R_1 and R_2 are the inlet and outlet reflection coefficients, phase-shifted to the nozzle throat,

$$R_1 = R_{in} \exp(-2\pi i f \frac{L_{in}}{c_1(M_1+1)}) \exp(-2\pi i f \frac{L_{in}}{c_1(1-M_1)}) \quad , \tag{25}$$

$$R_2 = R_{out} \exp(-2\pi i f \frac{L_{out}}{c_2(M_2+1)}) \exp(-2\pi i f \frac{L_{out}}{c_2(1-M_2)}) \quad . \tag{26}$$

To solve the system of equations, the Fourier transform of the entropy wave is used and the matrix system is solved for each frequency.

Figure 6 shows the solution of the system of equations using non-reflecting boundary conditions at the inlet and at the outlet, and the effect of using the outlet boundary condition R_{out} of Eq. 3. The solution shows a strong disagreement between the analytical model and the experimental results, and at the same time the importance of the outlet reflection coefficient.

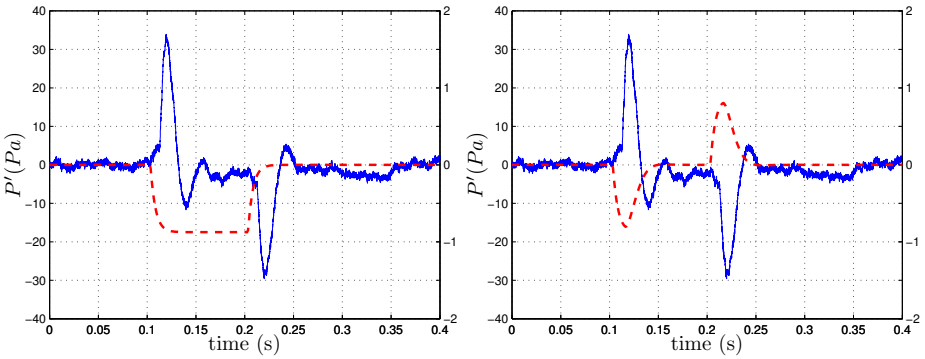

Figure 6. Experimental pressure signal obtained at the outlet compared to the analytical results. Solid line: Experimental data (left scale), Dashed line: Analytical method (right scale). Left: Non-reflecting outlet: Right: Partially reflecting outlet

To study this disagreement, an analysis of the compact nozzle assumption should be done. As stated before, the hypothesis is strictly valid only for the limit of infinite wavelength (zero frequency). In this case

it has been used for small but non-zero frequencies. Leyko *et al.*[10] showed that the hypothesis gives correct results for frequencies up to $\Omega = 0.2$ in the case of supersonic nozzles and subsonic convergent nozzles, but the case of a subsonic convergent divergent nozzle has never been treated. It is therefore important to perform this analysis because the analytical equations obtained with the compact nozzle hypothesis take into account only inlet to outlet relations (Eqs. 18-20), regardless of the flow evolution through the nozzle. In the case studied in this paper, the inlet and outlet Mach numbers are low, but the nozzle Mach number is not. A strong acceleration/deceleration is being produced inside the nozzle that the analytical model cannot take into account due to the limited description of the mean flow contained in the equations. Bake *et al.*[2] already suggested that the analytical model could not be used. To study the validity of the hypothesis, a numerical code called SNozzle[8] will be used. The code solves the linearised Euler equations of Eqs. 5-7 in the frequency domain, imposing the incoming waves at the inlet and at the outlet, and using non reflecting boundary conditions. Using the code, we can verify if the compact nozzle solution can still be used for non-zero frequencies in this type of nozzles. The direct and indirect noise ratios have been plotted in Fig. 7 as a function of frequency for the EWG nozzle geometry. The indirect noise ratio is defined as the out-coming acoustic wave (w_2^+) generated by an incoming unitary entropy wave (w_1^s), and the direct noise ratio is the out-coming acoustic wave (w_2^+) generated by an incoming unitary acoustic wave (w_1^+). It can be seen that the compact nozzle solution is correct for the limit of small frequencies, but at the same time that indirect noise ratio increases fast as non-zero frequencies are considered. From $\Omega \approx 0.03$ to the maximum frequency of the signal ($\Omega \approx 0.077$), the indirect noise ratio is 20 times higher than the one predicted using the compact nozzle hypothesis, making it impossible to use the analytical method. When considering zero-frequency, the entropy wave entering the nozzle generates a strong acoustic wave in the convergent, and another one in the divergent. These two waves have opposite phases due to the mean flow acceleration term in Eq. 6 (which is positive in the convergent, and negative in the divergent). Both waves cancel out at the outlet when they are added up, giving a small global contribution (due only to the global acceleration between the inlet and the outlet, but where the strong accelerating effect of the convergent is cancelled by the decelerating effect of the divergent). When a non-zero frequency wave is considered, the phase-shift of both waves is not exactly π as the propagation of the waves through the nozzle has to be taken into account. Due to this change of phase, the two strong acoustic waves do not cancel out completely, generating an extra contribution due to the convergent-divergent effect. This extra contribution cannot be modelled by the compact nozzle method, as it takes into account only the global acceleration between the inlet and the outlet. This effect does not occur when the flow is only accelerated (or only decelerated).

Bake *et al.*[2] developed an analytical method to solve the wave propagation through the convergent divergent nozzle. This method, still based in the compact nozzle hypothesis, is explained and discussed as an appendix.

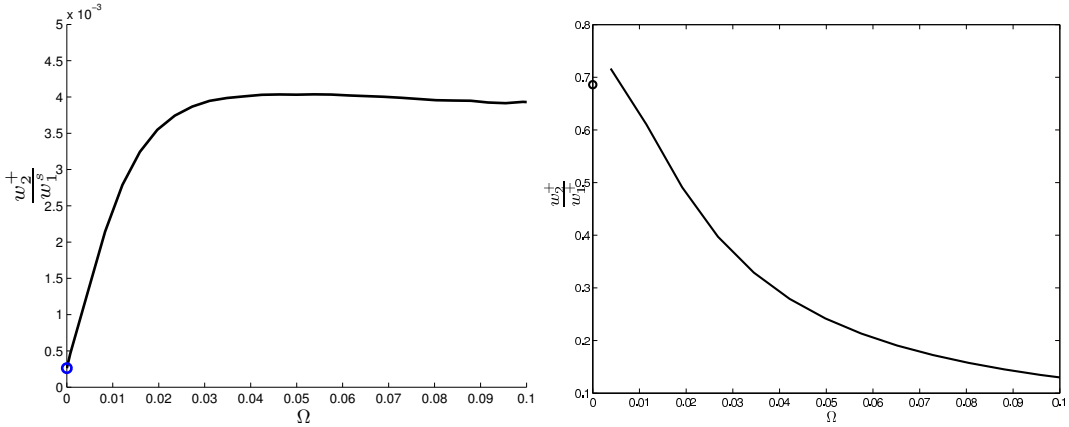

Figure 7. Left: indirect noise ratio. Right: Direct noise ratio. Dot: Marble and Candel solution. Solid line: SuperNozzle.

V. Waves generated by the heating device

In the EWG experiment, the heating device placed at the inlet can be modelled as a source term in the energy equation. To use analytical methods to study the propagation of entropy waves through the nozzle, the source term has to be decomposed in entropy and acoustic waves. For the supersonic case it was shown that the noise generated is due only to the entropy wave of the heating device.[9] In the subsonic case it has been considered that the acoustic waves generated by the heating device can be neglected.[3,7] In this section an analysis of the two mechanisms of noise generation will be performed to understand the source of the noise measured at the outlet. To obtain the acoustic and entropy waves generated by the heating device a simple 1D model will be used in the configuration illustrated in Fig 8: it takes into account the fluctuating heat release of the heating device Q', the waves and the mean flow (it should be noticed that the mean flow is constant through the device, and therefore $M_0 = M_1$).

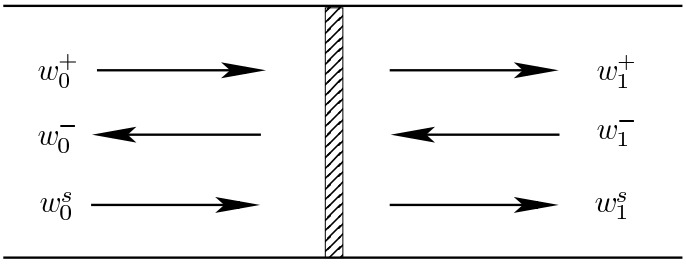

Figure 8. Waves definition through the heating device

As the heating device is short compared to the wavelength of the waves, the compact hypothesis will be used here, as done by Leyko *et al.*[10] for the compact one dimensional cold flame. Considering zero mean heat release ($Q = 0$), the conservation equations for the mass, enthalpy and entropy perturbations can be written between the inlet and the outlet as,

$$\left(\frac{\dot{m}'}{\dot{m}}\right)_0 = \left(\frac{\dot{m}'}{\dot{m}}\right)_1 \quad , \tag{27}$$

$$\left(\frac{T_t'}{T_t}\right)_0 + \frac{T_0}{T_{t0}}q' = \left(\frac{T_t'}{T_t}\right)_1 \quad , \tag{28}$$

$$\left(\frac{s'}{C_p}\right)_0 + q' = \left(\frac{s'}{C_p}\right)_1 \quad , \tag{29}$$

where q' is a non dimensional form of the fluctuating heat release: $q' = Q'/(\dot{m}_0 C_p T_0)$. The mass, total temperature and entropy perturbations can be written as a function of the primitive variables p', u' and s' using Eq. 12-14. With the definition of the acoustic and entropy waves of Eqs. 15-17, the three jump conditions can be written,

$$(1+\frac{1}{M_1})w_0^+ + (1-\frac{1}{M_1})w_0^- - 2w_0^s = (1+\frac{1}{M_1})w_1^+ + (1-\frac{1}{M_1})w_1^- - 2w_1^s \quad , \tag{30}$$

$$\left[(1+M_1)w_0^+ + (1-M_1)w_0^- + \frac{2(w_0^s+q')}{\gamma-1}\right] = \left[(1+M_1)w_1^+ + (1-M_1)w_1^- + \frac{2w_1^s}{\gamma-1}\right] \quad , \tag{31}$$

$$w_0^s + q' = w_1^s \quad . \tag{32}$$

The acoustic and entropy waves generated by the device can be calculated from these equations when considering no incoming waves,

$$w_h^s = q' \quad , \tag{33}$$

$$w_h^+ = \frac{M_0}{M_0+1}q' \quad , \tag{34}$$

$$w_h^- = \frac{M_0}{1-M_0}q' \quad . \tag{35}$$

Knowing that the inlet Mach number is small, one is tempted to neglect the acoustic waves compared to the entropy waves, as the ratio between them is very small (approximately 0.035). To see if direct noise can be neglected, a detailed study should be done to analyse the influence of each wave in the global noise generated at the outlet. Doing an order of magnitude analysis, the ratio between indirect and direct noise in the EWG can be estimated. This ratio is calculated using the entropy to acoustic wave ratio generated by the heating device with the indirect and direct noise ratios as follows,

$$\eta = \underbrace{\left[\frac{w^+_{2,ind}}{w^s_h}\right]}_{\text{Indirect noise}} \times \underbrace{\left[\frac{w^s_h}{w^+_h}\right]}_{\text{Wave Ratio}} \times \underbrace{\left[\frac{w^+_{2,dir}}{w^+_h}\right]^{-1}}_{\text{Direct Noise}} . \tag{36}$$

The first term is the indirect noise ratio, obtained analytically or using Fig 7, the second is the entropy to acoustic wave ratio generated by the heating device, calculated dividing Eqs. 33 and 34, and the third one is the inverse of the direct noise ratio, calculated analytically or using Fig. 7. The indirect to direct noise ratio is frequency-dependant. In the case of the EWG geometry, with the physical parameters shown in Table. 2, the indirect to direct noise ratio is plotted in Fig. 9. It can be seen that the ratio is smaller than one for the frequency range of interest ($\Omega = 0 - 0.088$), and therefore direct noise is significant and cannot be neglected.

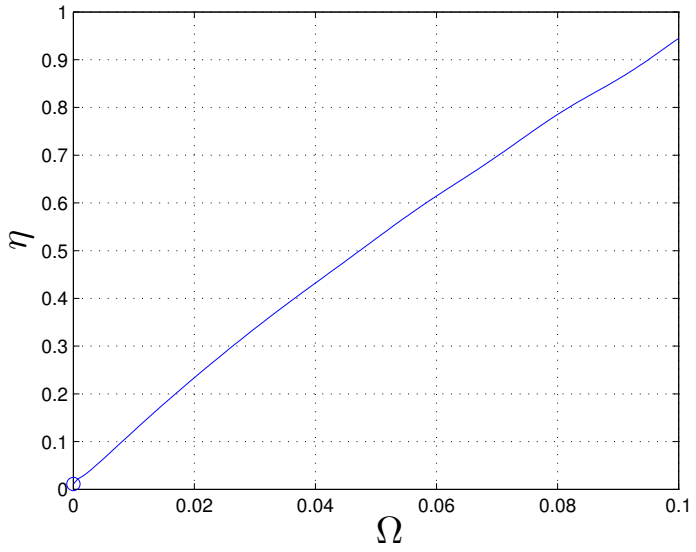

Figure 9. Indirect to direct noise ratio. Dot: Analytical solution. Solid line: SNozzle solution

It can be shown that this is not the case for the supersonic case,[9] where the indirect to direct noise ratio is $\eta \approx 15$, and direct combustion noise can be neglected.

VI. Semi-analytical method

To solve the LEE through the nozzle, the code SNozzle will be used. The idea is to calculate the transfer functions of the waves through the nozzle in the 'SNozzle domain' plotted in Fig 1. These transfer functions, defined as the out-coming waves generated by a unitary incoming wave are calculated using non reflecting boundary conditions in all boundaries. Combining the incoming and out-coming waves, we obtain nine transfer functions, namely,

$$\left[\frac{w^-_1}{w^+_1}\right] \quad , \quad \left[\frac{w^-_1}{w^s_1}\right] \quad , \quad \left[\frac{w^-_1}{w^-_2}\right] \quad , \tag{37}$$

for the upstream propagating acoustic wave,

$$\left[\frac{w_2^+}{w_1^+}\right] \quad , \quad \left[\frac{w_2^+}{w_1^s}\right] \quad , \quad \left[\frac{w_2^+}{w_2^-}\right] \quad , \tag{38}$$

for the entropy wave, and,

$$\left[\frac{w_2^s}{w_1^+}\right] \quad , \quad \left[\frac{w_2^s}{w_1^s}\right] \quad , \quad \left[\frac{w_2^s}{w_2^-}\right] \quad , \tag{39}$$

for the downstream propagating acoustic wave.

These transfer functions are frequency-dependant. To calculate them, three set of simulations were performed using SNozzle. In each one, a wave is introduced to calculate the out-coming ones:

- **Entropy**: w_1^s
- **Acoustic Inlet**: w_1^+
- **Acoustic Outlet**: w_2^-

For each set of simulations, a frequency sampling was done. In this way each SNozzle simulation has a single unitary incoming wave at a single frequency and the transfer functions of Eqs. 37-39 can be calculated as a function of frequency.

The results obtained are used to solve the EWG problem with all the waves and the reflection coefficients. To do so, the linear property of the LEE solution is used to write,

$$w_1^- = \left[\frac{w_1^-}{w_1^+}\right] \cdot (w_1^+ + w_h^+) + \left[\frac{w_1^-}{w_1^s}\right] \cdot w_1^s + \left[\frac{w_1^-}{w_2^-}\right] \cdot w_2^- \quad , \tag{40}$$

$$w_2^+ = \left[\frac{w_2^+}{w_1^+}\right] \cdot (w_1^+ + w_h^+) + \left[\frac{w_2^+}{w_1^s}\right] \cdot w_1^s + \left[\frac{w_2^+}{w_2^-}\right] \cdot w_2^- \quad , \tag{41}$$

The entropy wave w_1^s and the acoustic wave w_h^+ are the known source terms of the indirect and direct noise generation. The acoustic wave generated by the heating device is calculated as a combination of both acoustic waves of Eq. 34 and 35 using the inlet reflection coefficient, namely,

$$w_h^+ = w_0^+ + R_1 \cdot w_0^- = \left(\frac{M}{M+1} + R_1 \frac{M}{1-M}\right) w^s \quad . \tag{42}$$

It should be noticed that R_1 is the reflection coefficient at the nozzle inlet, and therefore it should take into account the effect of the settling chamber. Writing the acoustic waves at the inlet and at the outlet as $w_1^+ = R_1 \cdot w_1^-$ and $w_2^- = R_2 \cdot w_2^+$, two extra equations are obtained. The system can be re-arranged in a matrix form as,

$$\begin{bmatrix} R_1 & -1 & 0 & 0 \\ 0 & 0 & -1 & R_2 \\ 0 & \left[\frac{w_2^+}{w_1^+}\right] & \left[\frac{w_2^+}{w_2^-}\right] & -1 \\ -1 & \left[\frac{w_1^-}{w_1^+}\right] & \left[\frac{w_1^-}{w_2^-}\right] & 0 \end{bmatrix} \begin{bmatrix} w_1^- \\ w_1^+ \\ w_2^- \\ w_2^+ \end{bmatrix} = \begin{bmatrix} 0 \\ 0 \\ -\left[\frac{w_2^+}{w_1^s}\right] \\ -\left[\frac{w_1^-}{w_1^s}\right] \end{bmatrix} w^s + \begin{bmatrix} 0 \\ 0 \\ -\left[\frac{w_2^+}{w_1^+}\right] \\ -\left[\frac{w_1^-}{w_1^+}\right] \end{bmatrix} w_h^+ \quad . \tag{43}$$

The matrix and the source terms are all frequency-dependant, therefore the system has to be solved using the Fourier transform of the signal. The pressure signal is recomposed with the acoustic waves at the outlet.

A. Reflection coefficients

The analytical method solves the propagating problem in the 'Analytical Domain' of Fig 1. This means that the boundary conditions have to replace the physical phenomena not captured in the study.

For the outlet boundary condition, the study was already done for the numerical simulation (Section III), and the reflection coefficient obtained (R_{out}). This reflection coefficient is phase-shifted to the nozzle throat as done in Section IV.

The inlet boundary condition has to be, on the other hand, studied in detail. R_1 is calculated from R_{in} with a phase-shift, but no experimental data exist for this coefficient. In the supersonic case Leyko *et al.*[9] used both $R_{in} = 0$ and $R_{in} = -1$, showing that the reflection coefficient had little influence in the results. This is due to two main reasons: Firstly the flow is supersonic, and therefore waves reflected at the outlet cannot propagate back to the inlet region. Secondly, direct noise is negligible in the supersonic configuration, and the upstream propagating acoustic wave generated by the heating device can be neglected. This is not the case of the subsonic case, where the acoustic waves are significant. From Eq. 42 it can be seen that the reflection coefficient has a significant importance in the source term of the propagation equations. Unfortunately, no experimental data exists from the inlet reflection coefficient. An analytical approximation is here proposed to take into account the settling chamber in the reflection coefficient.

The conservation equations across the section change between the settling chamber (SC) and the inlet (0) of the nozzle (Fig. 1) can be written as,

$$S_{sc} \cdot u'_{sc} = S_0 \cdot u'_0 \quad , \tag{44}$$

$$p'_{sc} = p'_{sc} \quad , \tag{45}$$

considering low Mach number both at the settling chamber and at the nozzle inlet. In this way, two relations can be written between the waves at the settling chamber and at the heating device tube, namely,

$$w^+_{sc} - w^-_{sc} = \Gamma(w^+_0 - w^-_0) \quad , \tag{46}$$

$$w^+_{sc} + w^-_{sc} = w^+_0 + w^-_0 \quad , \tag{47}$$

where $\Gamma = \frac{S_0}{S_{sc}}$ is the ratio between sections. R_{in} is defined as the relation between the downstream propagating wave and the upstream propagating one. It reads,

$$R_{in} = \frac{w^+_0}{w^-_0} = \frac{(\Gamma - 1) + R_{sc}(1 + \Gamma)}{(1 + \Gamma) + R_{sc}(\Gamma - 1)} \quad . \tag{48}$$

R_{sc} is the reflection coefficient at the inlet of the settling chamber, where a mass flow rate is imposed, therefore $R_{sc} = 1$.

B. Results

The experimental data is reproduced for Reference Test Case 2 of[3] (mean flow properties are shown in Table 2). The semi-analytical method is compared to the experimental data. A good agreement is obtained in pressure shape and amplitude (though the amplitude is slightly over-predicted).

After the validation of the semi-analytical method using the Reference Test Case, several configurations were tested and compared with the experimental data.[2] In Fig 11 the maximum pressure fluctuation was compared to the experimental data for several nozzle Mach numbers, giving a correct agreement up to Mach 0.7. It should be noticed that both direct and indirect combustion noise are taken into account to reproduce the experimental curve, as well as the inlet and outlet reflection coefficients. The ratio between both mechanisms of combustion noise generation varies with the nozzle Mach number: Indirect noise tends to zero when the Mach number is low and increases as the flow is accelerated.

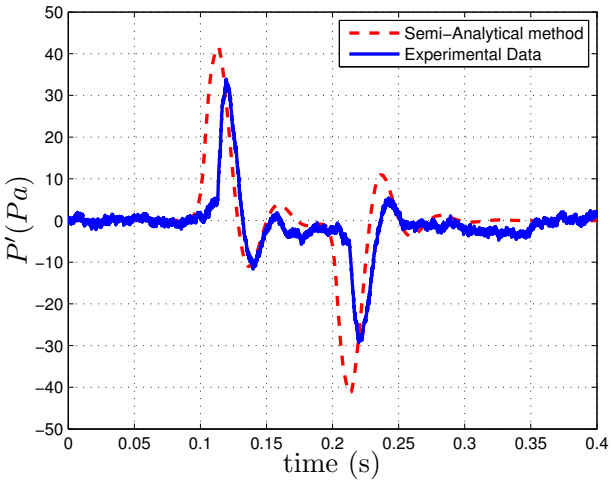

Figure 10. Pressure signal measured at the outlet for Reference Test Case 2 (Mach 0.7 at the throat). Dashed line: Semi-Analytical method solving both direct and indirect combustion noise. Solid line: Experimental data

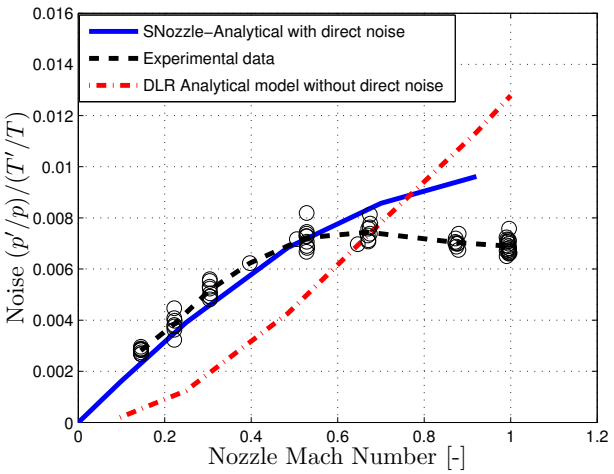

Figure 11. Evolution of the noise peak at the outlet of the EWG as a function of the throat Mach number. Experimental data, semi-analytical method and analytical method proposed at the DLR.

VII. Conclusions

The subsonic case of the EWG experiment has been studied analytically and numerically. It has been shown that direct noise has an important effect in the global noise generated. The noise measured at the outlet comes both from direct and indirect noise generation, plus the reflection at the boundaries of the experimental set-up. The fully analytical model has been shown able to predict the propagating characteristics of the nozzle at zero frequencies, but at the same time it was seen that the results are limited to very low frequencies due to the effect of the combined acceleration/deceleration of the mean flow. This configuration of successive stages of acceleration and deceleration of the mean flow is present in axial turbo-machines, and therefore a detailed study of this cases should be made to analyse the possible errors made when using the compact nozzle hypothesis to calculate the noise at the outlet of aero-engines. A semi-analytical method based on the transfer functions of the nozzle solved using a harmonic quasi-1D LEE code (SNozzle) has been used to solve the propagation through the nozzle without the compact nozzle hypothesis with a strict separation of direct and indirect noise and taking into account the inlet and outlet reflection coefficients. This method has shown correct results for the reference test case studied and for a wide range of throat Mach numbers. Using a first order analysis of the waves generated by the heating device it has been shown that, for the subsonic case, direct noise is significant in the experimental set-up. This results differs from the choked case[9] where

indirect noise dominated direct noise.

Appendix

To study the subsonic convergent divergent nozzle, a method was proposed by Bake *et al.*[2] to solve analytically the propagation using the compact nozzle hypothesis without the limitations of the Marble and Candel theory. This method is based in the division of the nozzle as two subsonic nozzles, one convergent and another one divergent. To solve the propagation of the waves, the quasi-transfer functions of the nozzle is calculated separately for the convergent and for the divergent and the propagation is studied sequentially. This combination of transfer functions is coupled: the noise generated in the convergent depends on the reflection of the waves in the divergent, and vice versa. To solve the system of equations, Bake *et al.*[2] neglected the upstream propagating acoustic wave generated in the divergent (by entropy and acoustic waves). In this way the system of equations is no longer coupled. The quasi-transfer functions obtained can be written in the non-dimensional form using the Marble and Candel method (Eqs. 9-11) between the inlet (1) and the nozzle throat (T) for the convergent, and between the throat and the outlet (2) for the divergent. In the case of the convergent they read,

$$\frac{w_T^+}{w_1^+}[AA] = \frac{2M_T}{1+M_T}\frac{1+M_1}{M_1+M_T}\frac{1+[(\gamma-1)/2]M_T^2}{1+[(\gamma-1)/2]M_T M_1} \quad , \tag{49}$$

$$\frac{w_T^+}{w_1^s}[SA] = \frac{M_T-M_1}{1+M_T}\frac{M_T}{1+[(\gamma-1)/2]M_T M_1} \quad , \tag{50}$$

$$\frac{w_T^s}{w_1^s}[SS] = 1 \quad , \tag{51}$$

and similarly for the divergent, replacing the inlet and throat subscripts for the throat and the outlet respectively. In dimensional form Eqs. 49-51 are equivalent to Eqs. 1-4 of.[2] The pressure wave at the outlet generated by the entropy wave is calculated combining the transfer functions,

$$\frac{w_2^+}{w_1^s} = \underbrace{\frac{w_T^+}{w_1^s}[SA]\cdot\frac{w_T^+}{w_1^+}[AA]}_{\text{Convergent}} + \underbrace{\frac{w_T^s}{w_1^s}[SS]\cdot\frac{w_3^+}{w_T^s}[SA]}_{\text{Divergent}} \tag{52}$$

The first term is the acoustic wave generated in the convergent which is obtained by the combination of two terms: the indirect noise generation in the convergent, and the propagation of this noise through the divergent. The second term is the indirect noise generated in the divergent, which is obtained combining the propagation of the entropy wave through the convergent with the indirect noise generation in the divergent.

This method provides the results shown in Fig 11. It should be noticed that, for this analysis, direct combustion noise and reflecting boundaries were not taken into account.

As stated before, the upstream propagating acoustic wave inside the nozzle has been neglected. It can be shown that this wave is significant and has to be included in the analysis. This wave, generated by entropy and acoustic waves propagating through the divergent, generates acoustic waves in the convergent section which will propagate downstream contributing to the total noise. To solve the problem, Eq. 9-11 can be written between the inlet (1) and the nozzle throat (T), and from the nozzle throat to the outlet (2). We obtain,

$$\left(\frac{\dot{m}'}{\dot{m}}\right)_1 = \left(\frac{\dot{m}'}{\dot{m}}\right)_T = \left(\frac{\dot{m}'}{\dot{m}}\right)_2 \quad , \tag{53}$$

$$\left(\frac{T_t'}{T_t}\right)_1 = \left(\frac{T_t'}{T_t}\right)_T = \left(\frac{T_t'}{T_t}\right)_2 \quad , \tag{54}$$

$$\left(\frac{s'}{C_p}\right)_1 = \left(\frac{s'}{C_p}\right)_T = \left(\frac{s'}{C_p}\right)_2 \quad . \tag{55}$$

If the upstream propagating acoustic wave is not neglected, the method should give the same solution as the analytical solution of Marble and Candel. This occurs because the method proposed is still based on the compact nozzle hypothesis (even if it is applied to two separate elements, the method considers that the distance between them is zero, and the compact nozzle hypothesis could be applied to the whole system). A different solution would be obtained if the distance between the convergent and de divergent is considered different to zero. This last method was tested in the frame of this work, but was found to be too dependant on the considered length.

References

[1]C. Bailly, C. Bogey, and S. Candel. Modelling of sound generation by turbulent reacting flows. *International Journal of Aeroacoustics*, 9(4):461–490, 2010.

[2]F. Bake, N. Kings, A. Fischer, and Rohle I. Experimental investigation of the entropy noise mechanism in aero-engines. *International Journal of Aeroacoustics*, 8(1-2):125–142, 2008.

[3]F. Bake, C. Richter, B. Muhlbauer, N. Kings, I.Rohle, F.Thiele, and B.Noll. The entropy wave generator (ewg): a reference case on entropy noise. *Journal of Sound and Vibration* , pages 574–598, 2009.

[4]T. Colonius, S.K. Lele, and P. Moin. The sound generated by a two-dimensional shear layer: The far field directivity from computations and acoustic analogies. *Computational Aeroacoustics*, 219, 1995.

[5]N. A. Cumpsty and F. E. Marble. The interaction of entropy fluctuations with turbine blade rows; a mechanism of turbojet engine noise. *Proc. R. Soc. Lond. A* , 357:323–344, 1977.

[6]M. E. Goldstein. A generalized acoustic analogy. *J. Fluid Mech.* , 488:315–333, 2003.

[7]M. S. Howe. Indirect combustion noise. *J. Fluid Mech.* , 659:267–288, 2010.

[8]N. Lamarque and T. Poinsot. Boundary conditions for acoustic eigenmodes computation in gas turbine combustion chambers. *AIAA Journal* , 46(9):2282–2292, 2008.

[9]M. Leyko, F. Nicoud, S. Moreau, and T. Poinsot. Numerical and analytical investigation of the indirect noise in a nozzle. In *Proc. of the Summer Program* , pages 343–354, Center for Turbulence Research, NASA AMES, Stanford University, USA, 2008.

[10]M. Leyko, F. Nicoud, and T. Poinsot. Comparison of direct and indirect combustion noise mechanisms in a model combustor. *AIAA Journal*, 47(11):2709–2716, November 2009.

[11]M. J. Lighthill. On sound generated aerodynamically. i. general theory. *Proc. R. Soc. Lond. A , Mathematical and Physical Sciences*, 211(1107):564–587, 1952.

[12]F. E. Marble and S. Candel. Acoustic disturbances from gas nonuniformities convected through a nozzle. *Journal of Sound and Vibration* , 55:225–243, 1977.

[13]B. Muhlbauer, B. Noll, and M. Aigner. Numerical investigation of the fundamental mechanism for entropy noise generation in aero-engines. *Acta Acustica united with Acustica 95*, pages 470–478, 2009.

[14]T. Poinsot and S. Lele. Boundary conditions for direct simulations of compressible viscous flows. *J. Comput. Phys.* , 101(1):104–129, 1992.

[15]T. Poinsot and D. Veynante. *Theoretical and Numerical Combustion*. R.T. Edwards, 2nd edition, 2005.